DETAILED EXAMINATION OF DEFORMATIONS INDUCED BY INTERNAL HYDROGEN EXPLOSIONS: PART 2 MODELS.

O. HALIM, E. STUDER, S. KOUDRIAKOV, B. CARITEAU, A. BECCANTINI
DEN/DM2S, CEA, Université Paris-Saclay, FRANCE

ABSTRACT

In industries handling hydrogen, explosion is feared because of its effects on people and property. In the nuclear industry, such explosion during the course of severe accidents can challenge the integrity of containment, which is the last barrier against releasing radioactive materials into the environment. The Three Mile Island accident in the United States in 1979 and more recently the Fukushima accident in Japan had highlighted the importance of this phenomenon for a safe operation of nuclear installations and during accident management. In 2013, the French Research Agency (ANR) launched the MITHYGENE project with the main aim of improving knowledge on hydrogen risk for the benefit of reactor safety. In this project, one of the areas of work concerned the effect of hydrogen explosions. In this context, CEA carried out a test program with its SSEXHY facility and CFD computational analysis with the EUROPLEXUS code to build a database on deformations of simple structures following an internal hydrogen explosion. Different regimes of explosion propagation have been studied from detonation to slow deflagration. Different targets were tested such as plates of variable thickness and cylinders. Detailed instrumentation was used to obtain data for the validation of coupled CFD models of combustion and structural dynamics. In this validation work, a step-by-step approach was adopted, starting by validating the target boundary conditions with quasi-static tests. Then, the dynamics of the structures were studied in a decoupled manner and finally in a coupled manner with the treatment of the propagation of the explosion in the tube. A companion article details the experimental set-up and the results obtained. This article now focuses on the comparison between experimental results and the numerical ones obtained using CFD models.

KEYWORDS: Combustion loading, Fluid Structure Interaction, Europlexus.

1.0 INTRODUCTION

In chemical and process industries handling hydrogen or during certain postulated accidents in nuclear reactor containment, hydrogen gas can be released into an industrial building or into the reactor containment. The Three Mile Island accident in the United States in 1979 and more recently the Fukushima accident in Japan had highlighted the importance of this phenomenon for a safe operation of nuclear installations and during accident management. Depending on the local concentration and/or presence and activation of mitigation devices, hydrogen may burn following different combustion regimes. These regimes may include jet fires, slow deflagrations, fast deflagrations or detonations depending on the combustion process development. Thus, one has to estimate the severity of a combustion process under given geometrical configuration, scale, and composition of combustible mixture.

One of the main questions is to predict/estimate the explosion effect on the integrity of a building and on different material inside. In terms of numerical modeling, the one way coupling approach is widely used nowadays for simulation of these phenomena. The fluid domain is modelled by a CFD code using fixed grid in space and the obtained pressure distribution is space and its evolution in time is used as a boundary condition for a structural dynamics code in order to compute the structural behavior. This uncoupled approach neglects the impact of the structural motion on the fluid variables and this deficiency should be quantified in order to improve the predictive character of numerical codes. Recently, some efforts have been made to take into account the structure deformation in combustion simulations; the works of [1] and [2] can be consulted for examples of Fluid Structure Interaction (FSI) modeling.

In order to validate and further improve the FSI models in EUROPLEXUS code [3], an R&D program initiated in the framework of the MITHYGENE project [4]. A middle-scale facility called SSEXHY (Structure Subjected to and EXplosion of Hydrogen) has been built at CEA and an experimental program is been conducted to produce detailed data on simple structure deformations loaded by various hydrogen combustion regimes. An accompanying article [5] details the experimental set-up and the results obtained. In the present article we shall focus on the comparison between the experimental data and the results obtained using the FSI models implemented in the EUROPLEXUS code.

2.0 PHYSICAL AND NUMERICAL MODELING

A thorough description of FSI algorithms and methods available in EUROPLEXUS code have been given in [2] (and references therein). In this document we only briefly describe the governing equations and numerical schemes which were used for code validation given in the next section.

Structural subdomain

The numerical modeling in the structural subdomain is performed using a Lagrangian formulation. The conservation of momentum equation also called the dynamic equilibrium is given by [2]

$$\int_V \delta\mathbf{v}^T \rho \frac{\partial \mathbf{v}}{\partial t} dV + \int_V tr((\nabla \partial \mathbf{v})^{\boldsymbol{T}} \cdot \boldsymbol{\sigma}\, dV - \int_V \delta\mathbf{v}^T \rho \boldsymbol{f}_b dV - \int_S \delta\mathbf{v}^T \mathbf{t}\, dS = 0 \qquad (1)$$

where ρ is the density of the control volume V having boundary surface S, $\mathbf{v}$ and $\partial\mathbf{v}$ are the vectors of velocities and virtual velocities at a point (x,y,z) within V, $\boldsymbol{\sigma}$ is the Cauchy stress, $\nabla\partial$v is the spatial gradient of the virtual velocity vector, $\mathbf{f}_b$ are the volumetric forces per unit mass and $\mathbf{t}$ are the boundary surface tractions. Finite element discretization is applied to the Equation 1 which leads to the following equation

$$\boldsymbol{Ma} = \boldsymbol{F}^{\text{ext}} - \boldsymbol{F}^{\text{int}} \qquad (2)$$

where $\boldsymbol{M}$ is the lumped mass matrix, $\boldsymbol{a}$ is the vector of nodal accelerations, $\boldsymbol{F}^{ext}$ are the external forces and $\boldsymbol{F}^{int}$ are the internal forces. The above equation is solved using explicit in time finite difference scheme.

Fluid subdomain

The model used for validation is based on the RDEM (Reactive Discrete Equation Method) approach [6] which requires the solution of the reactive Riemann problem between the burnt and unburnt regions. The combustion model was described in details in [7] and here we present only essential details. The system of equations is the two-phase Euler equations including the transport equation for the progress variable ξ.

$$\frac{\partial}{\partial t}\xi + \boldsymbol{D}\nabla\xi = 0 \qquad (3)$$

This equation is in non-conservative form. The apparent velocity $\boldsymbol{D}$ needs to be defined only on the interface between reactants and combustion products (with the same value ahead and behind it) and represents its velocity. The apparent velocity is computed as a function of the fundamental flame speed K_0 via

$$\boldsymbol{D} = \boldsymbol{w} + K_0\boldsymbol{n} \qquad (4)$$

where $\boldsymbol{n}$ is the normal to the flame surface going from the burnt to the unburnt region, $\boldsymbol{w}$ is the velocity of the unburnt gas. We also suppose that we know the fundamental flame speed *Ko* as function of space

and time. Finally, the convective fluxes are discretized using the finite-volume framework and the second order Two-Shock method [8], and an explicit second order scheme in time is applied to the discretized in space equations.

3.0 NUMERICAL VALIDATION USING THE EXPERIMENTAL DATA

Brief description of relevant experimental data

A thorough description of the SSEXHY experimental facility, experimental protocols and associated results are presented in the companion article [5] ("Detailed examination of deformations induced by internal hydrogen explosions: Part 1 Experiments"). Here we briefly present the SSEXHY facility and the experimental data used in this paper for FSI model validation.

The SSEXHY combustion tube is a stainless steel obstructed duct designed to study the acceleration mechanisms of premixed hydrogen/air flames. The tube includes four interchangeable sections connected by flanges and in the present tests only three were used. Each section is 1310 mm long with an internal diameter of 120 mm. Two blank flanges can be used to seal the combustion tube at its extremities (Fig. 1). An array of equally spaced annular obstacles are placed inside the tube (BR=30% and spacing is equal to tube diameter).

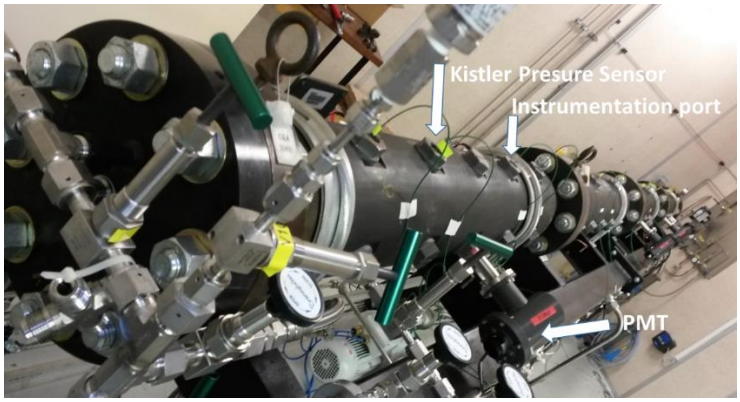

Figure 1. SSEXHY tube and associated instrumentation.

To investigate the effect of combustion loads on structures, the combustion tube is coupled with a FSI module. The connection between the combustion tube and the FSI module occurs at the end flange of the tube. Here, an intermediate flange that ensure the coupling replaces the end-sealing flange. A cylindrical adaptor (L=500 mm and internal diameter of 120 mm) is installed at the end flange of the tube at which a specimen for loading is attached (Fig. 2, left). A circular plate made of stainless steel 304L has the following dimensions: diameter D = 175 mm and a uniform thickness of 0.47 mm. This plate has been clamped between two flanges, the flange of the cylindrical adapter and the counter-flange, so that the visible diameter of the plate is reduced to 120 mm. Two gaskets in the form of O-ring has been installed at each side of the plate in order to assure the sealing when the nuts are tighten on the studs (Fig. 2, left). The Fluid-Structure Interaction (FSI) module is enclosed by a safety dome (Fig. 2, right). It is a stainless steel pressure vessel with an internal diameter of 700 m and a total length of 1900 mm, being designed for a nominal pressure of 8 bar.

Figure 2. Circular plate clamped between two flanges (left) and the safety dome (right).

The experiments have been performed using several hydrogen/air mixtures. In this paper only the experimental results corresponding to nearly stoichiometric mixture of air and hydrogen are considered for validation. The thermos-dynamic properties of the mixture are given in Table 1.

Table 1. Thermo-dynamic variables of hydrogen/air mixture used for validation (p_0 = 1 bar and T_0 = 300). Initial mixture composition: $xH_2+(1-x)/(n+1)\ (O_2+nN_2)$, n=79.1/20.9

Property	**Mixture 1**
x	0,295
P_{AICC} (bar)	8,00
P_{CJ} (bar)	15,58
c_{su} (m/s)	408,7
U_{CJ} (m/s)	1977
$U_{CJ,DEF}$ (m/s)	1008

Validation Methodology

The following strategy has been chosen for validation of the numerical models:

- The experimental data devoted to static pressure loading applied to the disc are used in order to choose the appropriate boundary conditions. An analytical solution available for the elastic region of the stress-strain diagram supposing that the material is perfectly homogeneous, is also used for comparisons.

- Once the boundary conditions are chosen, we perform computations of the plate deformation by applying the experimental pressure signal measured during the explosion tests where a *full* flange of the thickness 50 mm is installed at the end of the tube and a pressure transducer is placed in the middle of the flange. This constitutes a *decoupled* validation approach. Different stress-strain models are tested and compared to the experimental data corresponding to the deformed plate (disc).

- Finally, a fully-coupled computation, where the fluid part as well as the disc are meshed, and the numerical results are compared to their experimental counterparts. The boundary conditions and the stress-strain model were taken from the previously validated steps.

Static loading validation results

The computations of plate deflection under static pressure loadings have been performed using axi-symmetric geometry. The following properties provided by a manufacturer has been considered for the disc and the gasket:

Table 2. Plate and Gasket material properties.

	Plate	**Gasket**
Young's modulus, E(Pa)	1.66 E11	7.0E8
Poisson's ratio, ν	0.275	0.499
Radius, R (mm)	100.0	26.5
Thickness, h (mm)	0.47	1.5

We emphasize that the main difficulty in numerical modeling at this stage is to choose the physically relevant boundary conditions at the disc clamped edge. The following boundary conditions have been tested (Fig. 3):

- disc clamped edge with zero displacement (**BC1**) only visible part of the disc is taken into account;
- disc clamped edge with possible slip between the disc and the gasket, i.e. the corresponding mesh nodes are not connected and can move relative to each other (**BC2**) ;
- disc clamped edge with non-slip condition between the disc and the gasket but possible displacement, i.e. the corresponding mesh nodes are connected (**BC3**).

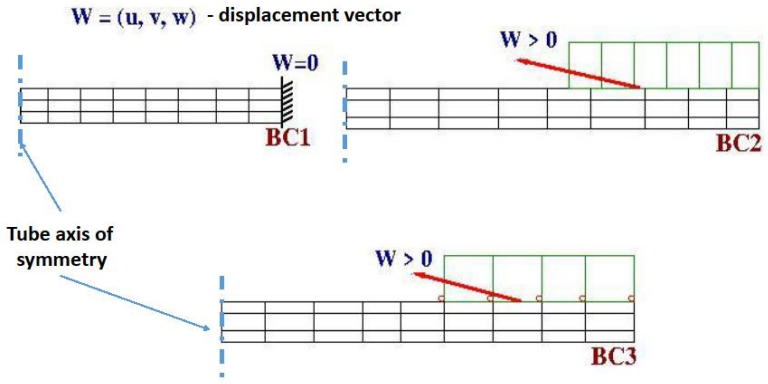

Figure 3. The sketch of the boundary conditions applied. Only the upper gasket is represented (green color). Clamped edge with zero displacement (**BC1**, top left); clamped edge with slip between the disc and the gasket (**BC2**, top right); clamped edge with non-slip between the disc and the gasket (**BC3**, bottom).

For all the tests we consider two-dimensional axisymmetric geometry with element size of h/4 = 0.1175 mm. Two in-house CFD computer codes were used: one is Cast3M code [9] and the other is EUROPLEXUS code [3]. The elastic isotropic model has been applied in both cases and a steady solution has been sought in the former case and an asymptotic solution obtained using time marching

scheme – in the latter case. An analytical solution based on linear elastic theory of plates is also presented on the Figures for comparison. This solution for the displacement, w, is available for the elastic region of the stress-strain diagram supposing that the material is perfectly homogeneous and its behavior agrees with the Hook's law (see [10] + references therein); it is given by

$$w = \frac{\Delta p}{64D}(R^2 - r^2)^2 \tag{5}$$

where $D = \frac{Eh^3}{12(1-\nu^2)}$, R = 60 mm and r is the radial coordinate.

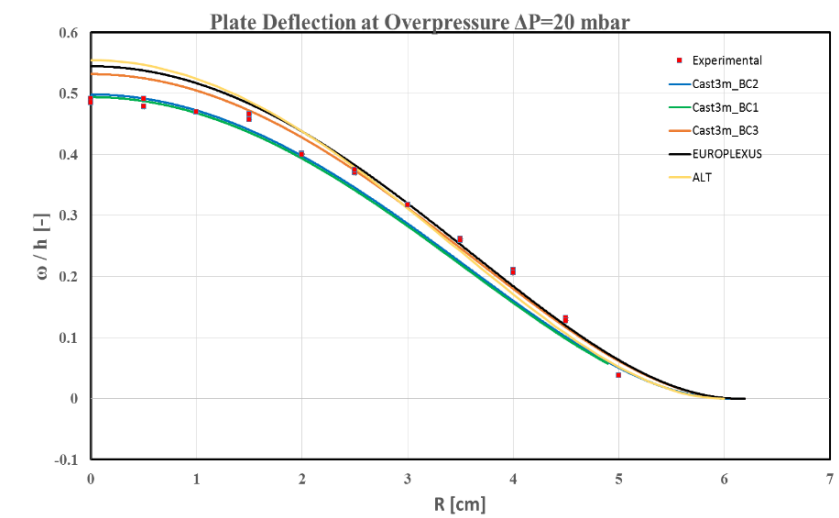

Figure 4. Plate deflection at relative overpressure of 20 mbar. **BC3** boundary condition is used for EUROPLEXUS solution. "ALT" = Analytical Linear Theory (yellow curve). The experimental data are represented by red dots.

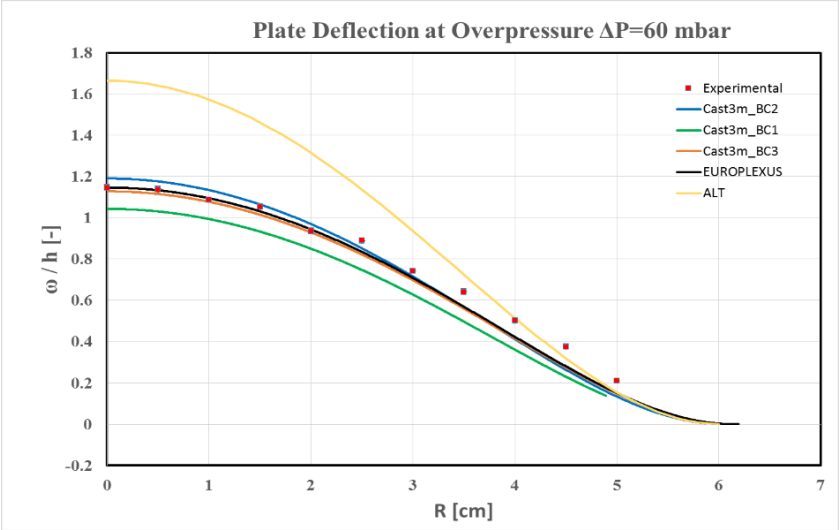

Figure 5. Plate deflection at relative overpressure of 60 mbar. **BC3** boundary condition is used for EUROPLEXUS solution. "ALT" = Analytical Linear Theory (yellow curve). The experimental data are represented by red dots.

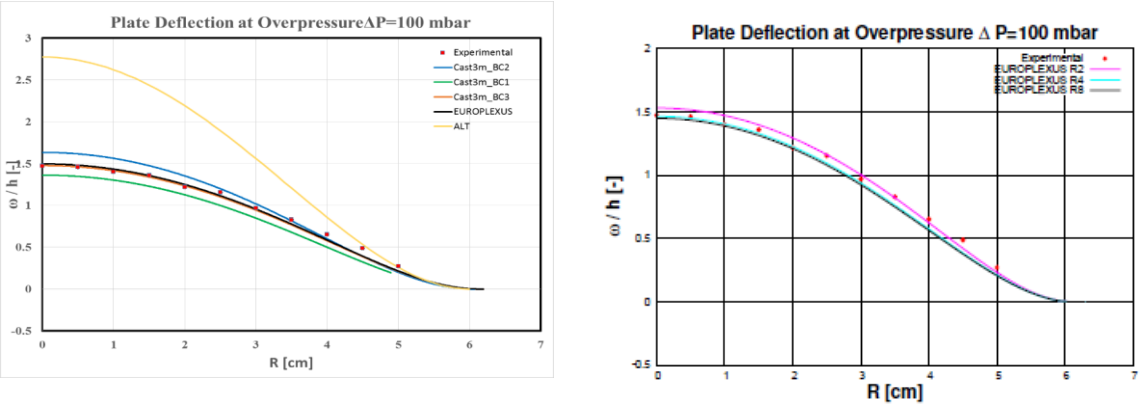

Figure 6. Plate deflection at relative overpressure of 100 mbar (left). **BC3** boundary condition is used for EUROPLEXUS solution: "ALT" = Analytical Linear Theory (yellow curve); the experimental data are represented by red dots. EUROPLEXUS solutions using different grids (right).

On the Figures 4-6 we present the computational results corresponding to numerically converged solutions corresponding to the overpressure values of 20 mbar, 60 mbar, and 100 mbar. The mesh convergence study using uniform mesh ant two cells, four cells and eight cells within the plate thickness (R2, R4 and R8 on Fig. 6, right) show that at least four cells have to be used in order to have converged solution. All presented results on the other figures correspond to the case R8. Three types of boundary conditions were tested using the Cast3M code and one type, BC3, is tested using the EUROPLEXUS code. The computed results are systematically compared with their experimental counterparts. The following observations can be made:

- the analytical solution based on linear elastic theory (yellow curve) gives acceptable results for small overpressure values, up to 20 mbar. Beyond that value it largely over predicts the experimental values due to the fact that underlying hypothesis are not met for relatively large overpressure values.

- the boundary condition **BC3** results in numerical solutions which are most close to the experimental data. This type of boundary condition will be applied for all the computations performed using the EUROPLEXUS code.

- the numerical solutions corresponding to Cast3M code and to the EUROPLEXUS code with the same initial and boundary condition (**BC3**) are very close to each other. The small difference between them can be explained by the difference in spatial (quadratic vs linear elements) discretization.

Decoupled dynamic loading validation results

The experimental data for this validation step are obtained with pressure signals recorder for rigid walls. Pressure sensors were installed along the adapters and at the center of the massive end-flange. The raw pressure signals are presented on the Figure 7. We can see that the experimental pressure levels are rather high and one needs to perform an additional analysis. Experimentally, our pressure sensors are screwed directly on the instrumentation ports without any damping material. Consequently, the measurements gather information coming from the fluid as well as from the structure itself. A simple analysis can be performed in order to find the bounding cut-off frequencies. A frequency of 750 Hz corresponds to the sound wave travelling back and forth along

a 4 m long steel tube, while a frequency of 60000 Hz corresponds to the sound wave travelling back and forth across the tube wall width.

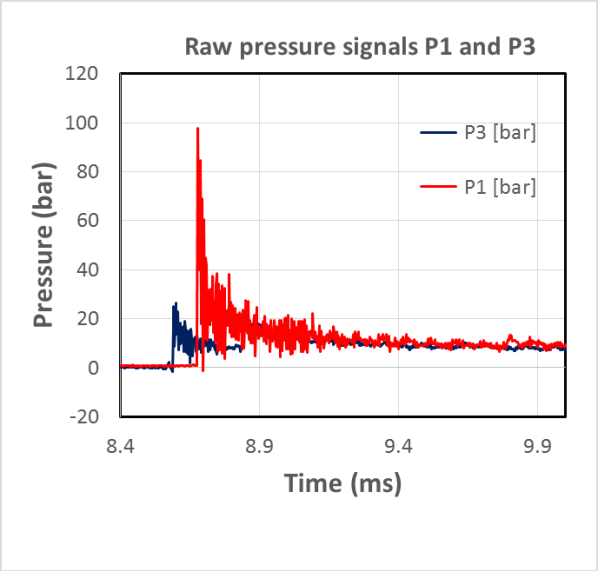

Figure 7. Experimentally obtained pressure signals at the end flange (P1, red curve) and at the adapter wall, 15cm from the end flange (P3, blued curve).

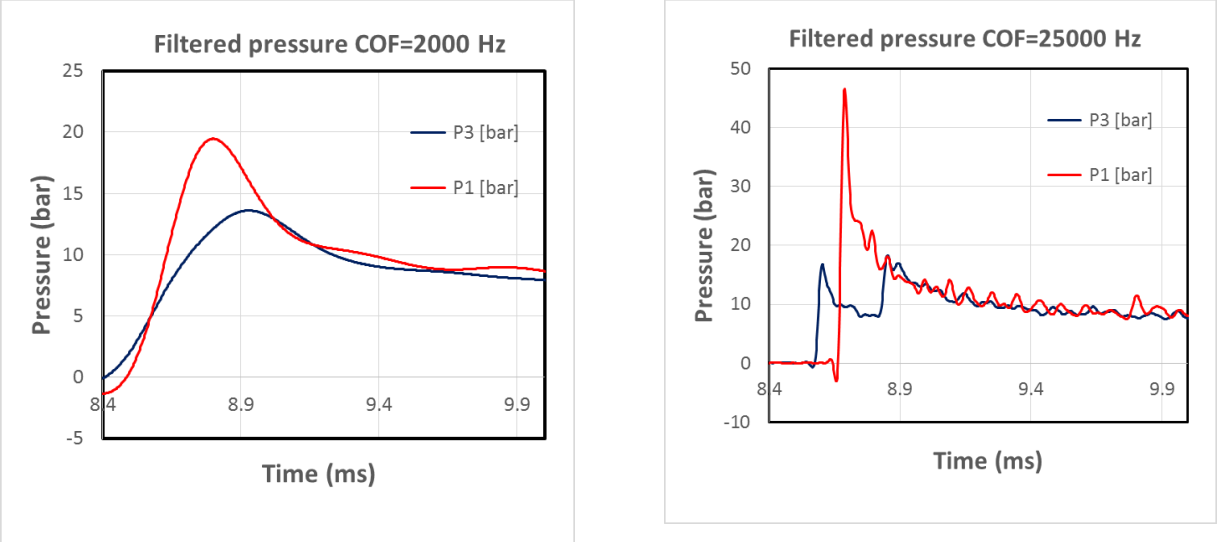

Figure 8. Filtered experimental pressure signals P1 and P3 with the cut-off frequency of 2000 Hz (left) and 25000 Hz (right).

We have analyzed the dependence of the impulse and the maximum pressure value on the cut-off frequency. The analysis showed that the impulse is weakly dependent on the cut-off frequency and it stabilizes after 10000 Hz while the maximum pressure value represents a growing function of cut-off frequency, as expected.

The numerical solutions show rather weak dependence on cut-off frequency. The large variations however were observed while using different stress-strain models, like Von Mises isotropic model, Von Mises dynamic model with different model parameters [3].

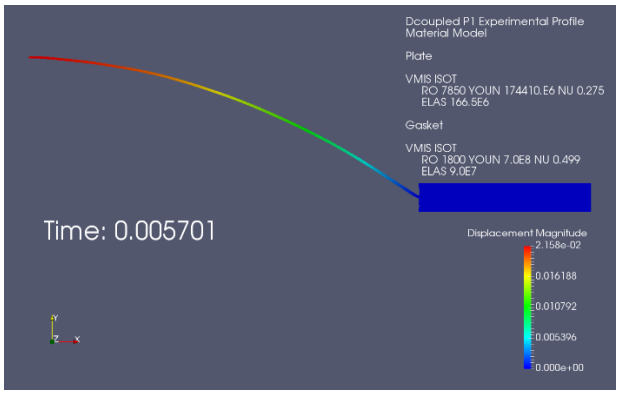

Figure 9. Typical solution obtained using one way coupling approach; the state at t=5.7 ms.

The same number of elements as in the static loading simulations were used in the present validation step. The boundary conditions of type **BC3** were applied at the clamped edge of the disc. The pressure evolution corresponding to the raw pressure signal (presented here) or to a filtered pressure signal is uniformly applied at the lower part of the disc. A typical solution is presented on the Fig. 9: the deformation of the disk takes place almost instantly after the arrival of the detonation wave followed by the high frequency oscillations propagating along the disc surface and having relatively small amplitude. This behavior will be compared to the experimentally measured behavior in the near future.

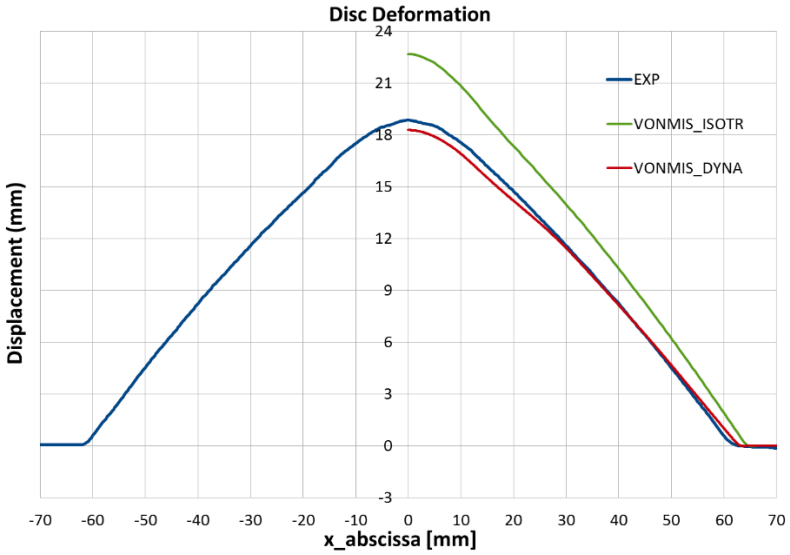

Figure 10. Comparison between the experimentally measured disc deformation (blue curve) and the numerical data obtained using Von Mises isotropic model (green curve) and Von Mises dynamic model (red curve).

As was mentioned earlier, the numerical solution varies greatly with different choice of behavior model. This can be seen on the Figure 10 where we compare the experimentally measured disc deformation along the plane of symmetry and the numerical solution for displacement obtained using the Von Mises isotropic and Von Mises dynamic models. The solution corresponding to the dynamic model is the closest to the experimental data. Moreover, this solution gives almost identical to the experimental data initial slope. The "dynamic" solution was obtained using the model constants D = 12000 and P = 4.4. This constants were experimentally obtained and described in [11]. We mention that the Von Mises dynamic model constants are not unique and we have tested the model constants coming from different references [12]. The results of this model-sensitivity analysis is presented on Figure 11. First of all, we

can see that the solution corresponding to the dynamic model with parameters D = 1.E+5 and P = 1.0 (yellow curve) is identical to the isotropic model, as expected because the dynamic models degenerates to the isotropic model for the above parameters, see Equation 6. This equation is the well-known Cowper-Sysmonds material

$$\frac{\sigma_{dyn}}{\sigma_{sta}} = 1 + \left(\frac{\dot{\varepsilon}}{D}\right)^{1/p} \tag{6}$$

where σ_{dyn} is the dynamic yield stress, σ_{sta} is the static yield stress, $\dot{\varepsilon}$ is the strain rate, D and p are constants.

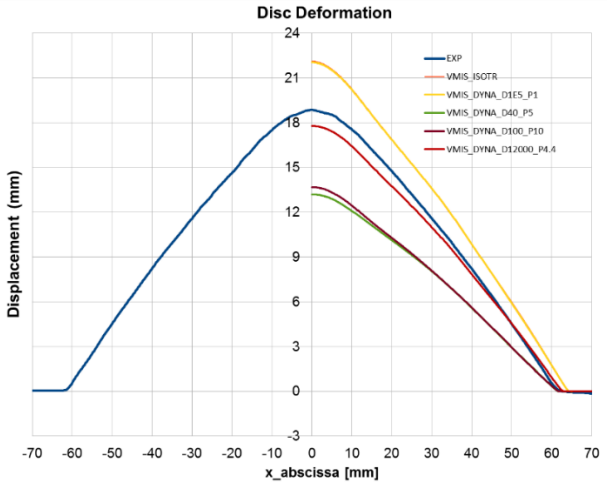

Figure 11. Comparison between the experimentally measured disc deformation (blue curve) and the numerical data obtained using Von Mises isotropic model (orange curve) and Von Mises dynamic model with different parameters (the other curves).

Secondly, the solution which is closest to the experimental data is given by the dynamic model with the model parameters D = 12000 and P = 4.4. Therefore these model parameters will be considered for the fully coupled computations.

Fully coupled dynamic loading validation results

The final validation step corresponds to the fully coupled numerical analysis. The whole length of the SSEXHY tube has been meshed as well as the plate and gaskets. Same number of elements was taken in the plate thickness as in the previous validation steps. The element size inside the fluid domain was

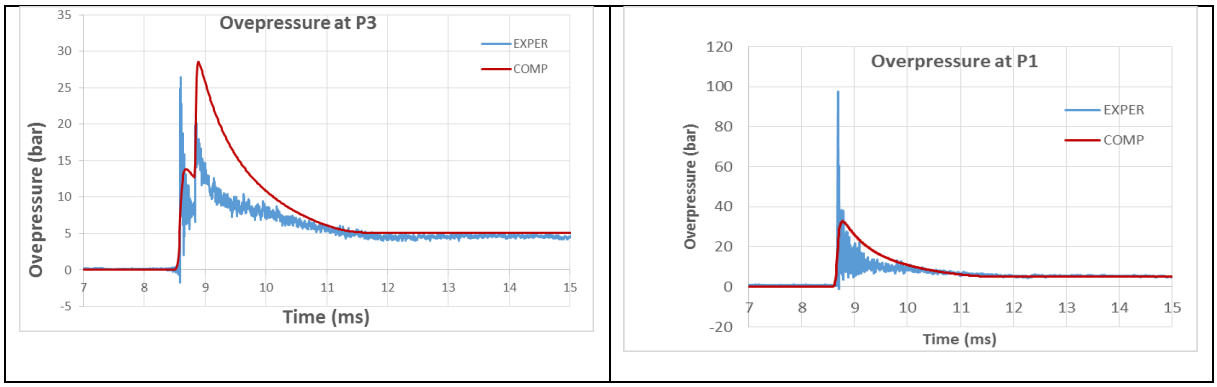

Figure 12. Comparison between the experimentally measured pressure evolutions (blue curves) and the numerically modelled pressure evolution (red curves, shifted in time) at P3 (left) and P1 (right).

larger and equal to approximately 5 mm. The Arbitrary Lagrangian-Eulerian method (ALE) [13] was employed for the FSI computation where the fluid grid was following the motion of the solid. Preliminary tests with infinitely rigid end flange were performed and we compared thus obtained pressure signals with the experimental results (Fig. 12). The numerical solution is not affected by high frequencies typical for experimental signals; the first computed pressure peak at P3 is close to the theoretical Chapman-Jouget value of 14.6 bar and the asymptotic behavior is very close to the behavior of the experimental evolution.

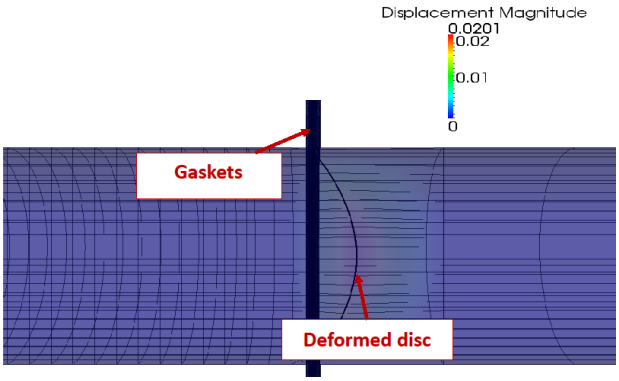

Figure 13. Zoomed numerical solution for disc displacement at t=3 ms.

The zoomed part of the numerical solution representing disc deformation soon after the arrival of the detonation wave is shown on the Figure 13. We can see that the fluid grid follows the motion of the deformed disc. The final solution (at t= 5 ms) over predicts the deformation level compared to the experimental data (Fig. 14). The maximum relative difference is equal to 9.4%. We attribute this difference to two factors: a) the difference in overpressure between the experimental and computational results, and b) the smaller number of elements along the disc radius compared to the decoupled approach. As a next step, we are going to perform simulations using embedded mesh method FSI algorithms [2]. This method uses a Lagrangian formulation for the structure and Eulerian formulation for the fluid, where the two subdomains are discretized independently of each other: this will allow us to use similar (to the decoupled case) number of elements along the disc radius.

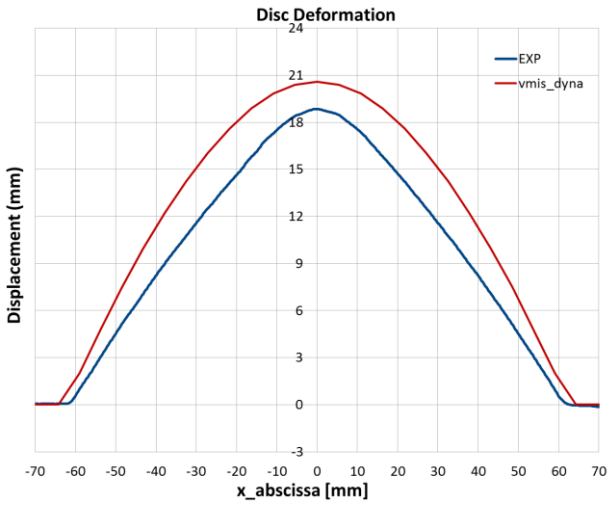

Figure 14. Comparison between the experimentally measured disc deformation (blue curve) and the numerical data obtained using fully coupled technique: RDEM model for fluid and Von Mises dynamic model for solid. ALE method is applied for FSI.

4.0 CONCLUSIONS

In this paper we describe validation work based on detonation tests performed in SSEXHY facility coupled with a metal disc. A step-by-step approach was adopted, starting by validating the target boundary conditions with quasi-static tests. This allowed us to identify the boundary condition at the disc clamped edge where non-slip condition between the disc and the gasket and possible displacement are enforced. This boundary condition resulted in the numerical solution close to its experimental counterpart. Then, the dynamics of the structures were studied in a decoupled manner. Different stress-strain models were tested and the Von Mises dynamic model with specific parameters shown to be the best candidate for further analysis and computations. Finally, a fully coupled approach with the treatment of a) the propagation of the explosion in the tube (RDEM model) and FSI coupling with application of Von Mises dynamic model for the structures was performed. The differences between the experimental data and the numerical solutions are explained and the additional simulations are planned in order to improve the results. Additionally, the future CFD validation work will be based on experimental tests performed using different hydrogen/air mixtures.

REFERENCES

1. A. Kotchourko, A. Lelyakin, and T. Jordan, "Modeling of hydrogen flame dynamics in narrow gap with bendable walls," presented at the 7th International Conference on Hydrogen Safety (ICHS2017), Hamburg, Germany, 2017.
2. V. Aune, E. Fagerholt, M. Langseth, and T. Borvik, "A shock tube facility to generate blast loading on structures," *Int. J. Prot. Struct.*, vol. 7, no. 3, pp. 340–366, 2016.
3. EUROPLEXUS software. http://www-epx.cea.fr/
4. MITHYGENE project. https://www.irsn.fr/EN/Research/Research-organisation/Research-programmes/Mithygene-project/Pages/MITHYGENE-project.aspx
5. Author1, Author2,…"Detailed examination of deformations induced by internal hydrogen explosions: Part 1 Experiments"
6. A. Beccantini and E. Studer , "The reactive Riemann problem for thermally perfect gases at all combustion regimes". *International Journal for Numerical Methods in Fluids*, 2009.
7. A. Velikorodny et al., "Combustion modeling in large scale volumes using EUROPLEXUS code", Journal of Loss Prevention in Process Industries, **35**, pp. 104-116 (2015)
8. E. F. Toro, "Riemann Solvers and Numerical Methods for Fluid Dynamics", Springer 1997.
9. Cast3M code. http://www-cast3m.cea.fr/
10. R. Scarpa, « Mécanisme d'accélération d'une flame de prémélange hydrogène/air et effets sur les structures », PhD Thesis, l'Université d'Orléans, 2017.
11. Le Maoult A. Caractérisation en traction du matériau Z3 CN 18-10 à diffÃ c rentes vitesses de sollicitations. Technical report, CEA DMT/SEMT/LISN/RT/99-097/A. 1999
12. Forrestal and Sagartz 1978, Elastic-Plastic Response of 304 Stainless Steel Beams to Impulse Loads, J. Appl. Mech 45(3), 685-687 (Sep 01, 1978)
13. T. Hirth, A. Amsden, J. Cook., "An Arbitrary Lagrangian-Eulerian computing method for all flow speeds", *J. Comp. Physics* (1974) 14.